Genetic Algorithm-Based Fast Real-Time Automatic Mode-Locked Fiber Laser

Guoqing Pu, Lilin Yi, *Member, IEEE*, Li Zhang, and Weisheng Hu, *Member, IEEE*

***Abstract*— The nonlinear polarization evolution-based passively mode-locked fiber laser is attracting increasing attention that can be attributed to its variety of operating regimes. However, the precise polarization tuning required to achieve these different regimes and the extreme vulnerability of these lasers to environmental disturbances have substantially hindered their widespread applications. Here, we experimentally demonstrate the first genetic algorithm-based real-time automatic mode-locked fiber laser, in which the fitness functions for the different regimes are based on temporal information only and where a modified genetic algorithm is proposed to accelerate the mode-locking time. The laser demonstrates an outstanding time-consumption performance, particularly when searching the second-order harmonic mode-locking regime and the Q-switching regime.**

***Index Terms*— Genetic algorithm, real-time, mode locking, ultrafast laser.**

I. Introduction

MODE-LOCKED fiber lasers (MLFLs) are widely applied in both scientific research and engineering in the generation of ultrashort pulses, which are used extensively in a wide range of applications [1]. Because of their rather simple setup and outstanding pulse quality, nonlinear polarization evolution (NPE)-based artificial saturable absorbers are widely adopted among the numerous approaches used to realize MLFLs [1]. Via polarization tuning, NPE-based passive MLFLs can realize various regimes, including the fundamental mode-locking (FML) regime, harmonic mode-locking (HML) regimes, and even the Q-switching (QS) regime. However, NPE-based MLFLs are reliant on polarization tuning, thereby making them extremely vulnerable to environmental disturbances, e.g., strain and thermal instabilities [2], [3]. In addition, because their polarization solution space is far narrower than that for the FML regime, locking onto the rarer regimes such as the HML regimes and the QS regime through manual polarization tuning processes is rather difficult.

To resolve these problems, automatic mode-locked lasers based on programmable polarization control by virtue of adaptive algorithms and electric polarization controllers (EPCs) have gradually emerged. Several automatic mode-locking researchers have reported the use of EPCs to sweep the polarization space directly [4]–[6]. However, this method offers quite low efficiency when the large polarization space is taken into consideration. Machine learning has contributed to the development of a self-tuning laser through birefringence classification [7], [8]. An intelligent laser enabled by a human-like algorithm that is capable of locking onto multiple regimes automatically has also been demonstrated [9]. Additionally, the genetic algorithm (GA) is a particularly favorable global optimization algorithm for use in automatic mode-locking research and several works have presented GA-based automatic mode-locking via polarization searching procedures [2], [3], [10]–[12].

The GA is a classic global optimization algorithm that was inspired by the evolution of living organisms [13]. The GA has a natural strength in that it avoids sticking at a local optimum, thus benefiting from its complex genetic operations. However, in previous GA-enabled automatic mode-locking researches, the fitness functions have been complex and thus it proved difficult to integrate the GA into a real-time setup. For example, second harmonic generation was used as a fitness function in a nonlinear BaB_2O_4 (BBO) crystal [10]. In addition, fitness functions that involved the optical spectrum [3], [11] and even a compound fitness function that used a temporal waveform, the optical spectrum and the electrical spectrum [2] have also been demonstrated. Therefore, off-line processing using a computer and measurement equipment would be required and the processes of automatically locating and locking onto the FML regime and the other rare regimes would become quite time-consuming. To illustrate this problem, the automatic mode-locking time for the FML regime is around 30 min [2], [10] and may even range up to 2 h when searching the HML regimes [12]. In addition, it is difficult to design a portable and low-cost automatic mode-locking fiber laser when using computer-based off-line control. To address this problem, we propose different fitness functions for different regimes where all fitness functions are based solely on temporal information, including the fast Fourier transform (FFT) results calculated from the temporal waveform. Therefore, the input for feedback control becomes concise because only an analog-to-digital converter (ADC) is required. The entire feedback control process can be integrated within a real-time method, thereby substantially reducing the time costs of searching the desired regimes and thus significantly reducing the laser cost. Additionally, in traditional GA-based automatic mode-locking processes, the computing center must go through each generation of the calculation. However, the desired individuals that lead to the desired regime may appear during the middle generations. It would thus be pointless to run through the remaining generations of the calculations after the desired individuals emerged. To provide a further improvement in the time consumption performance, we modify the traditional GA by terminating the algorithm when the desired individuals appear. The proposed automatic MLFL powered using this real-time feedback control method benefits from the simple fitness functions and the modified GA and demonstrates excellent

Manuscript received October 31, 2019; accepted November 18, 2019. Date of publication November 20, 2019; date of current version January 2, 2020. This work was supported by the National Natural Science Foundation of China under Grant 61575122. *(Corresponding author: Lilin Yi.)*

The authors are with the State Key Laboratory of Advanced Optical Communication Systems and Networks, Shanghai Jiao Tong University, Shanghai 200240, China (e-mail: lilinyi@sjtu.edu.cn).

Color versions of one or more of the figures in this letter are available online at http://ieeexplore.ieee.org.

Digital Object Identifier 10.1109/LPT.2019.2954806

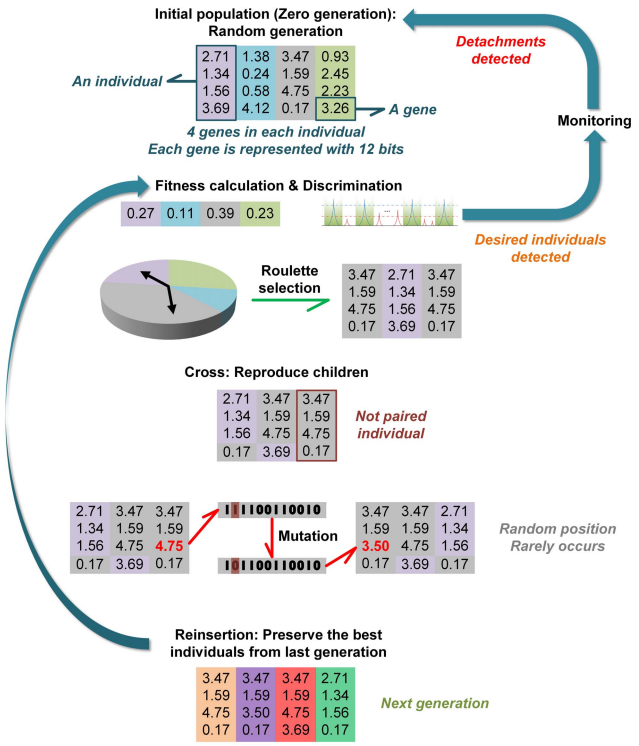

Fig. 1. Schematic of the proposed modified GA.

time consumption performance. The laser can locate onto the FML regime from the continuous wave (cw) state as rapidly as the previously reported laser powered by the advanced Rosenbrock searching (ARS) algorithm [9]. Further, the mean times required by the modified GA-based laser to reach the second-order HML regime and the QS regime from the cw state are approximately 2.5 times and 4.5 times faster, respectively, when compared with the ARS-based laser. We prove in this work that the GA provides a good solution for fast polarization searching in a real-time automatic mode-locked fiber laser.

II. Principles

Fig. 1 illustrates the proposed modified GA. In the beginning, the initial population (i.e., the zero generation) is generated randomly. Each individual consists of four genes that correspond to four channels of 0–5 V DC control voltages for the EPC. As determined by the resolution of the digital-to-analog converters (DACs) that control the EPC, each gene is represented using 12 bits. A fitness calculation is then executed for each individual. Unlike the traditional GA, the discrimination operation to judge whether or not the current waveform reaches the desired regime is performed simultaneously and the algorithm stops searching immediately when the desired regime is detected, thus significantly reducing the algorithm's running time. The laser then sequentially enters into the monitoring phase based on the discrimination operation. When detachment (i.e., when the laser detaches from the desired regime) is detected, the laser will automatically recover to the desired regime by launching the modified GA again (i.e., the entire recovery requires no manual involvement). A roulette selection process is used to select individuals from the previous generation to form the next generation and the probability of each individual being selected has a positive correlation with its fitness. The cross operation that occasionally occurs between individuals mimics the breeding process of genes to produce offspring. Note that some individual may not be paired in the cross operation because of the generation gap. Mutation is a particularly rare operation that is used to alter the value at some random position in a gene, thereby preventing the algorithm from sticking at a local optimum. To preserve the best individuals (i.e., the individuals with the highest fitness) from the previous generation, a reinsertion operation is conducted to produce the next generation.

To terminate GA optimization immediately when the wanted individuals emerge and to achieve real-time monitoring for detachment detection, accurate discrimination of the various desired regimes is crucial. Therefore, the modified GA is combined with our previously proposed discrimination criteria for the various regimes [9]. To discriminate the mode-locking regimes, use of the dual-region count (DRC) scheme is proposed. The temporal waveform is divided into two regions containing pulses and noise. In the ideal case, all pulses should appear in the middle of the pulse regions and a dynamic threshold (i.e., a threshold that is altered according to the maximum of the current sampled waveform) is established in these regions to count the desired pulses. The count in the pulse regions is a fixed number at a specified pulse train repetition rate. The noise regions are the margins between the pulse regions and there should be no pulses in the noise regions. However, higher harmonic generation (i.e., HML pulses) and environmental disturbances can render large-amplitude noises in these margins. Therefore, another dynamic threshold is set as the limit for the noise. When the noise in the margins surpasses the threshold, the current waveform will not be judged to be the desired mode-locking regime. The DRC scheme has proved to be highly efficient in the field. The waveform is evaluated as the mode-locking regimes (i.e., including both the FML regime and the HML regimes) when the DRC is satisfied because the different mode-locking regimes have different count results. Additionally, the fitness function for the FML regime is the average amplitude of the counted pulses derived from the feature where the mode-locked pulse train has an amplitude that is much larger than that of the cw state.

The fitness function of the n-th order HML regime is proposed by virtue of its FFT characteristics. It was found that the kn-th spectral lines are much stronger than the other spectral lines based on observation of the massive FFT results for the HML regimes. Increasing the proportion of all kn-th spectral lines on purpose therefore accelerates the process of approaching the n-th HML regime and thus the fitness function of the n-th HML is the proportion of the kn-th spectral lines. The fitness function and the discrimination of the QS regime are based entirely on the FFT results. Because of their lower repetition rate, the majority of the FFT spectral components of the QS regime are concentrated on low frequencies. Therefore, the fitness function of the QS regime is chosen to be the low-frequency proportion of the FFT result. The QS regime discrimination is achieved by setting a threshold for the fitness of this low-frequency proportion. The waveform is then judged to lie in the QS regime when the fitness exceeds a preset threshold.

The first GA-based real-time automatic MLFL is shown in Fig. 2. The cavity length of this fiber laser is approximately 33.5 m. A 980 nm laser pumps an 8 m erbium-doped fiber (EDF) that acts as the gain medium through a wavelength division multiplexer (WDM). A 3 dB optical coupler keeps half of the power inside the cavity for the oscillation,

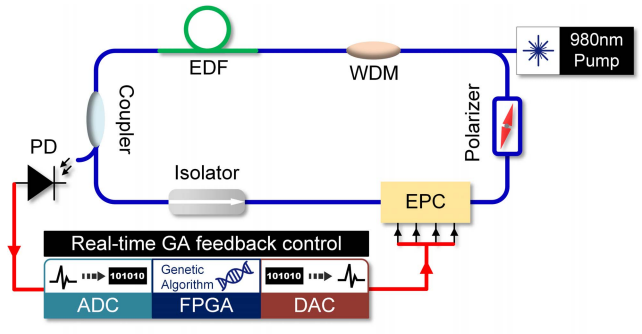

Fig. 2. GA-based real-time automatic MLFL setup.

while the other half is sent out for measurement and feedback. The isolator guarantees unidirectional running of the cavity. The EPC can respond in a matter of microseconds and is capable of generating all possible polarization states over the Poincaré sphere, where each set of voltages corresponds to a specific polarization state. The polarizer is the core component required in NPE-based mode locking to produce artificially saturated absorption. A 10 GHz photodetector (PD) is used to realize conversion from the optical domain to the electrical domain. The real-time GA feedback control system consists of a 400 MSa/s ADC with 8-bit resolution, a high-speed field-programmable gate array (FPGA) and four 100 MSa/s DACs with 12-bit resolution. Therefore, the size of the polarization space reaches 4096^4.

III. Results and Discussion

Using an identical setup, the laser can realize multiple operating regimes automatically, including the FML regime, the second-order HML regime, and the QS regime. Because there is no dispersion management operation inside the cavity, the laser operates under soliton mode-locking conditions with anomalous net dispersion. Fig. 3 illustrates various operating regimes under pump power of 600 mW. The frequency spectrum of the FML regime demonstrates a fundamental repetition rate of ~6.17 MHz, corresponding to a cavity length of ~33.5 m. Small Kelly sidebands can be observed in the corresponding optical spectrum. In the frequency spectrum for the second-order HML regime, it is obvious that the second spectral line is the strongest and corresponds to a repetition rate of ~12.34 MHz. The second spectral line is approximately 35.5 dB stronger than the fundamental repetition spectral line. In addition, the fourth, sixth, eighth and even the tenth spectral lines are all stronger than the odd-ordered spectral lines. Overall, the second-order HML frequency spectrum characteristics validate the effectiveness of the proposed fitness function for the HML regimes. Note that the proposed fitness and discrimination processes for the HML regimes are suitable for any order of HML regime. However, achieving higher order HML regimes requires an ADC with higher sampling rate. While the optical spectrum of the second-order HML regime is analogous to the optical spectrum of the FML regime, the former exhibits stronger Kelly sideband components. The repetition rate of the QS regime is shown to be approximately 120 kHz by its frequency spectrum. Moreover, the laser can switch smoothly among the different operating regimes by recording and setting the values of the EPC that have been experienced.

In the modified GA, the initial population size is set to be 20 and the maximum number of generations allowed

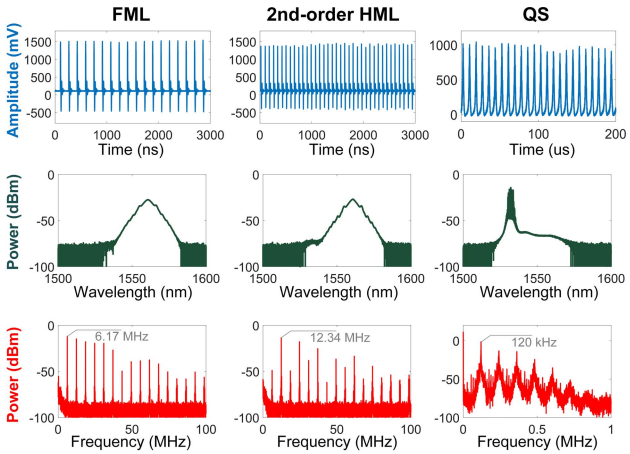

Fig. 3. Operating regimes. From left to right, the FML regime, the second-order HML regime, and the QS regime are shown. From top to bottom, oscilloscope traces, the optical spectra, and the frequency spectra are illustrated.

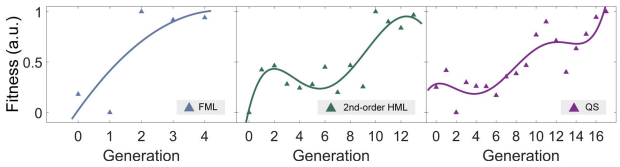

Fig. 4. Normalized average fitness optimization paths of the FML regime, the second-order HML regime, and the QS regime. The triangles indicate the recorded fitness values and the solid lines are the fitted polynomial curves.

in a single optimization is 100. It will skip the remaining generations when the desired regime is found. However, when the laser fails to lock onto the desired regime within 100 generations, the FPGA will re-run the modified GA using a different random initial population until the desired regime emerges. Because of the completely random process used for production of the initial population and the environmental fluctuations, the number of generations required to pass from the cw state to the same desired regime is usually different for each execution. Fig. 4 demonstrates one group of normalized average fitness paths for the FML regime, the second-order HML regime and the QS regime during optimization.

Obviously, the fitness gradually increases with increasing generations for the different regimes, thereby confirming the validity of our modified GA. However, the average fitness of each generation does not increase monotonically as it would in an ideal situation. The first reason for this behavior is the disturbances from the experimental environment. All experiments were conducted in an open environment without any thermal stability or vibration protection devices, thereby causing fitness variations for the same individual in different generations. In addition, the bias in the individual assessments performed using the mean value of three fitness calculations also contributes to these fluctuations in the average fitness curves. To evaluate each individual precisely, numerous fitness calculations are required to obtain a valid mean, but this procedure would be particularly time-consuming. Therefore, a trade-off must be determined between precise individual assessment and excellent time consumption performance. In the experiments, use of the mean value from three fitness calculations to evaluate the individuals is a middle choice that gives consideration to both sides of the trade-off. Additionally, it takes only

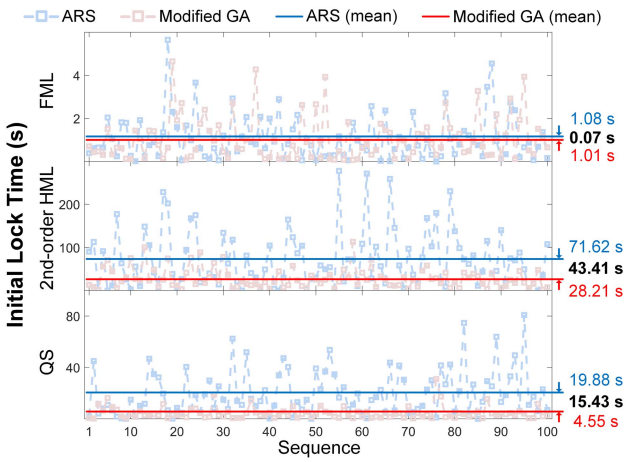

Fig. 5. Time-consumption performance comparison between the modified GA and the ARS. The squares on the dashed lines are the measured initial lock times and the solid lines indicate the mean time consumptions.

four generations (excluding the initial generation) to reach the FML regime. Because the polarization solution spaces of the rare regimes are much narrower than that of the FML regime inside the NPE-based MLFLs, it requires more than ten generations to lock onto the second-order HML regime or the QS regime. According to the experimental records, the fitness of the second-order HML regime and the QS regime illustrated have not yet converged when the second-order HML regime and the QS regime emerge due to the proposed new termination mechanism used in the modified GA. The modified GA stops the optimization process immediately when the desired regime is achieved thereby cutting off the subsequent convergence stage directly.

Fig. 5 shows a direct time consumption performance comparison between the modified GA and the ARS over 100 successive measurements. Note that the comparison experiments were conducted using an identical cavity and the same period. In this case, the initial lock time means the time cost from the cw state to the desired regime. The initial lock time is recorded precisely using a timer inside the FPGA that has a timing resolution of 3 ns. While the mean time consumption of the modified GA (1.01 s) when searching the FML regime is slightly faster than that of the ARS (1.08 s), this may be induced by environment disturbances such as drift. Therefore, we consider the modified GA and the ARS to perform equivalently in searching the FML regime. As illustrated in the middle part of Fig. 5, the modified GA is approximately 2.5 times faster in finding the second-order HML regime than the ARS. For the HML regimes and the QS regime, because of the complex FFT calculations required and the narrower polarization solution space available, it usually takes more time to reach the corresponding regime. In finding the second-order HML regime, the mean time consumption of the ARS was 71.62 s, while that of the modified GA was merely 28.21 s. Further, the ARS is approximately 4.5 times slower in locking onto the QS regime than the modified GA, with a mean time consumption of 19.88 s versus 4.45 s for the modified GA. In contributing to the powerful global optimization capacity, the modified GA shows superiority over the ARS in searching the rare regimes. Additionally, the time consumption variation of the ARS is greater than that of the modified GA (particularly in the second-order HML regime and QS regime cases). This is because of the ARS's sensitivity to the initial point. Because the ARS is a type of direct searching algorithm, the time consumption is principally determined by the positioning of the initial point. Overall, the proposed modified GA shows better time consumption performance than the ARS.

IV. Conclusion

In conclusion, we have experimentally demonstrated the first GA-based real-time automatic MLFL. The modified GA skips the remaining generations when the desired individuals have been detected via the proposed discrimination criteria. Benefitting from the simplified fitness functions that are merely based on temporal information, the modified GA can be integrated with a real-time feedback control system consisting of an ADC, an FPGA, and four DACs. Therefore, the laser can lock onto the FML regime, the second-order HML regime and the QS regime automatically using an identical setup and shows outstanding time consumption performance. In GA-based automatic mode-locking research, the laser can lock onto the FML regime with a mean time consumption of only 1.01 s in under 100 measurements. Furthermore, the time consumption performance when passing from the cw state toward the second-order HML regime and the QS regime is substantially improved when compared with the ARS. We believe that this powerful, portable and low-cost automatic MLFL will be useful in both scientific research and engineering applications.

References

[1] J. Kim and Y. Song, "Ultralow-noise mode-locked fiber lasers and frequency combs: Principles, status, and applications," *Adv. Opt. Photon.*, vol. 8, no. 3, pp. 465–540, Sep. 2016.
[2] R. I. Woodward and E. J. R. Kelleher, "Towards 'smart lasers': Self-optimisation of an ultrafast pulse source using a genetic algorithm," *Sci. Rep.*, vol. 6, Nov. 2016, Art. no. 37616.
[3] D. G. Winters, M. S. Kirchner, S. J. Backus, and H. C. Kapteyn, "Electronic initiation and optimization of nonlinear polarization evolution mode-locking in a fiber laser," *Opt. Express*, vol. 25, no. 26, pp. 33216–33225, 2017.
[4] G. Pu, L. Yi, L. Zhang, and W. Hu, "Programmable and fast-switchable passively harmonic mode-locking fiber laser," in *Proc. Opt. Fiber Commun. Conf. Expo.*, San Diego, CA, USA, Mar. 2018, pp. 1–3, Paper W2A.9.
[5] X. Shen, W. Li, M. Yan, and H. Zeng, "Electronic control of nonlinear-polarization-rotation mode locking in Yb-doped fiber lasers," *Opt. Lett.*, vol. 37, no. 16, pp. 3426–3428, 2012.
[6] T. Hellwig, T. Walbaum, P. Groß, and C. Fallnich, "Automated characterization and alignment of passively mode-locked fiber lasers based on nonlinear polarization rotation," *Appl. Phys. B, Lasers Opt.*, vol. 101, no. 3, pp. 565–570, 2010.
[7] X. Fu, S. L. Brunton, and J. N. Kutz, "Classification of birefringence in mode-locked fiber lasers using machine learning and sparse representation," *Opt. Express*, vol. 22, no. 7, pp. 8585–8597, 2014.
[8] T. Baumeister, S. L. Brunton, and J. N. Kutz, "Deep learning and model predictive control for self-tuning mode-locked lasers," *J. Opt. Soc. Amer. B, Opt. Phys.*, vol. 35, no. 3, pp. 617–626, 2018.
[9] G. Pu, L. Yi, L. Zhang, and W. Hu, "Intelligent programmable mode-locked fiber laser with a human-like algorithm," *Optica*, vol. 6, no. 3, pp. 362–369, 2019.
[10] U. Andral, R. S. Fodil, F. Amrani, F. Billard, E. Hertz, and P. Grelu, "Fiber laser mode locked through an evolutionary algorithm," *Optica*, vol. 2, no. 4, pp. 275–278, 2015.
[11] R. I. Woodward and E. J. R. Kelleher, "Genetic algorithm-based control of birefringent filtering for self-tuning, self-pulsing fiber lasers," *Opt. Lett.*, vol. 42, no. 15, pp. 2952–2955, 2017.
[12] U. Andral *et al.*, "Toward an autosetting mode-locked fiber laser cavity," *J. Opt. Soc. Amer. B, Opt. Phys.*, vol. 33, no. 5, pp. 825–833, 2016.
[13] J. H. Holland, "Genetic algorithms," *Sci. Amer.*, vol. 267, no. 1, pp. 66–73, 1992.